

## Fivefold-coordinated Ti<sup>4+</sup> in metamict zirconolite and titanite: A new occurrence shown by Ti K-edge XANES spectroscopy

FRANÇOIS FARGES

Laboratoire de physique et mécanique des géomatériaux, Université de Marne-la-vallée, URA CNRS 734 and LURE (and Stanford University), 2 rue de la butte verte, 93166 Noisy le Grand cedex, France

### ABSTRACT

The coordination environments of Ti in two fully metamict zirconolite samples and two partially metamict titanite samples were determined using high-resolution, X-ray absorption near-edge structure (XANES) spectroscopy at the Ti K edge. Fivefold-coordinated Ti is the dominant Ti species in the zirconolite samples ( $\sim 80 \pm 10\%$  of the total Ti atoms). This unusual Ti coordination is also possible in the titanite samples. No significant evidence for <sup>147</sup>Ti was found in any of the samples studied.

Comparison with other amorphous materials, such as other metamict minerals (aeschynite and pyrochlore) and titanosilicate glasses and melts, suggests that fivefold coordination is rather common for Ti<sup>4+</sup> in aperiodic structures. However, the metamict state is characterized by the presence of unusual trigonal bipyramids around <sup>151</sup>Ti<sup>4+</sup>.

### INTRODUCTION

Titanite and zirconolite (ideally CaTiSiO<sub>5</sub> and Ca-ZrTi<sub>2</sub>O<sub>7</sub>, respectively) are important phases in various crystalline titanate-phase assemblages proposed as nuclear waste forms (see Lutze and Ewing 1988; Ringwood et al. 1988). These phases can host significant amounts of high-activity radionuclides and, consequently, are subject to radiation damage (Ewing et al. 1987, 1995).

Metamict minerals such as zirconolite and titanite can be used to investigate the effect of radiation damage in these phases (Higgins and Ribbe 1976; Ewing et al. 1982; Fleet and Henderson 1985; Vance and Metson 1985; Lumpkin et al. 1986, 1991; Ewing et al. 1988; Hawthorne et al. 1991). Indeed, some natural actinide-bearing titanite and zirconolite become progressively amorphous to X-ray diffraction because of an increasing amount of defects that are mainly related to the  $\alpha$ -recoil atoms, displacing up to several thousands of atoms for each  $\alpha$ -decay event (Ewing et al. 1987, 1995).

To investigate the effects of radiation damage on the structure of metamict minerals, extended X-ray absorption fine-structure (EXAFS) spectroscopy has been used to probe the coordination environment around a variety of elements, such as Ti (Greegor et al. 1984a, 1984b; Lumpkin et al. 1986; Ewing et al. 1988; Hawthorne et al. 1991). In these studies, a decrease in the average Ti-O bond length between the crystalline and the metamict modifications was attributed to the presence of minor amounts of <sup>147</sup>Ti in the latter form. A complementary high-resolution, X-ray absorption near-edge structure (XANES) spectroscopy study at the Ti K edge in crystalline and metamict titanite and zirconolite is presented here. The advantage of the XANES method is its much greater sensitivity to the coordination environment of Ti. Indeed, an alternative in-

terpretation for the coordination of Ti in these metamict phases is proposed, which suggests, for the first time, the presence of major amounts of <sup>151</sup>Ti in the radiation-damaged portions of zirconolite (and possibly of titanite) and in several other complex metamict oxide minerals, such as aeschynite, pyrochlore, and euxenite.

### EXPERIMENTAL METHODS

#### Samples studied

Two natural samples of zirconolite from Sri Lanka were used in the present study (no. 111.35 from the Museum National d'Histoire Naturelle, Paris; no. B-20392 from the National Museum of Natural History, Washington, DC). These minerals have been described in detail elsewhere (Ewing et al. 1982; Lumpkin et al. 1986). These two Sri Lankan zirconolite specimens are black and fully amorphous in X-ray diffraction (XRD). They have received an accumulated radiation dose of up to 10<sup>26</sup>  $\alpha$ -decay events/m<sup>3</sup> over  $\sim 550$  m.y. [equivalent to about two displacements per atom (dpa)]. One chip of sample 111.35 was annealed at 1100 °C for 4 h in a platinum crucible in air, resulting in the crystallization of monoclinic zirconolite. These three zirconolite samples have also been studied at the Zr K, Th L<sub>III</sub>, and U L<sub>III</sub> edges (Farges et al. 1993).

Three titanite samples were selected (all from the Stanford University mineral collection). One is a crystalline, olive green sample of gem quality from Caperlibas, Minas Gerais, Brazil (sample no. 51,938). The other two are partially metamict: a slightly damaged titanite from Egansville, Ontario, Canada (referred to here as Egansville; no. 6,620), and a more damaged sample from an unknown locality in Ontario (referred to here as Ontario; no. 6,310). The latter two titanite specimens are black and opaque with

**TABLE 1.** Preedge parameters for selected Ti-bearing model compounds and crystalline and metamict zirconolite and titanite samples

	Avg. Ti coordination ( $\pm 0.1$ )	Preedge feature	
		Position (eV)	Normalized height*
$\text{Ni}_{2.6}\text{Ti}_{0.7}\text{O}_4$ (synthetic)	4	4969.7(1)	0.94(5)
$\alpha\text{-Ba}_2\text{TiO}_4$ (synthetic)	4	4969.5	1.00
$\text{K}_6\text{Ti}_2\text{O}_7$ (synthetic)	4	4969.7	0.93
$\text{Y}_2\text{TiMoO}_8$ (synthetic)	4	4969.9	0.74
$\text{Rb}_2\text{TiO}_3$ (synthetic)	4	4969.6	1.00
$\text{KNaTiO}_3$ (synthetic)	5	4970.6	0.73
$\text{Rb}_2\text{Ti}_4\text{O}_9$ (synthetic)	5	4970.5	0.47
$\text{K}_2\text{Ti}_2\text{O}_5$ (synthetic)	5	4970.6	0.51
Fresnoite (synthetic)	5	4970.6	0.65
$\text{Ba}_2\text{TiGe}_2\text{O}_8$ (synthetic)	5	4970.6	0.65
Rutile (Brittany)	6	4971.6	0.22
Anatase (synthetic)	6	4971.4	0.17
Perovskite (synthetic)	6	4971.4	0.11
Benitoite (California)	6	4971.2	0.04
Neptunite (California)	6	4971.1	0.32
Ilmenite (Brittany)	6	4971.7	0.22
$\text{TiZrO}_4$ (synthetic)	6	4971.2	0.21
<b>Titanite</b>			
Caperlibas (Brazil)	6	4971.4	0.18
Egansville (Canada)	5.9**	4971.3	0.22
Ontario (Canada)	5.7**	4971.1	0.27
Glassy (synthetic)	5.3**	4970.7	0.50
<b>Zirconolite</b>			
111.35 (annealed)	5.7	4970.9	0.17
111.35 (Sri Lanka)	5.1**	4970.4	0.39
B 20392 (Sri Lanka)	5.2**	4970.5	0.36

\* Using Si(311) on EXAFS4 beamstation (LURE). The full list of model compounds studied is in Farges et al. (1996a).

\*\* Estimated average Ti coordination based on crystalline zirconolite (see Fig. 5).

conchoidal cleavage. The XRD spectra for the two moderately radiation-damaged titanite samples still show a Bragg component (seven diffraction peaks observed for  $2\theta$  values between 20 and 60° in the Egansville titanite, but only three lines measured for the Ontario titanite). However, the X-ray diffuse-scattering component of the XRD pattern for these samples is significant: The intensity of the 311 line normalized to that for the diffuse scattering is ~40 and 10 for the Egansville and Ontario titanite samples, respectively (~70 for Caperlibas titanite). The samples are similar to those from other localities in Ontario (e.g., from the Cardiff mine), which are described in detail by Fleet and Henderson (1985), Hawthorne et al. (1991), and Lumpkin et al. (1991). These titanite samples are mostly from the Grenville Province of the Canadian Shield (~950 m.y. old). They have a low actinide content ( $\text{ThO}_2 + \text{UO}_2 \leq 0.1$  wt%), which produces a total radioactivity of ~0.3 mrad/s (calculated doses of  $\sim 2\text{--}3 \times 10^{25}$   $\alpha$ -decay events/ $\text{m}^2$ ; ~0.4–0.7 dpa; see Hawthorne et al. 1991; Lumpkin et al. 1991). Finally, a glass of titanite composition (referred to as glassy titanite) was synthesized by melting a sample of Caperlibas titanite at 1700 K for 4 h in a platinum crucible and quenching the melt by placing the bottom of the crucible in water.

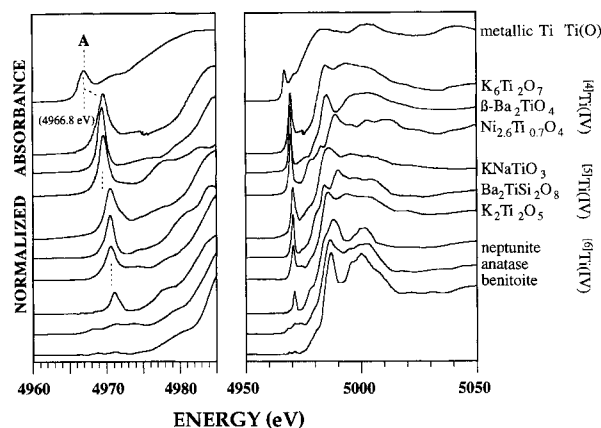


**FIGURE 1.** Ti *K*-edge XANES spectra collected for various model compounds. From top to bottom: metallic Ti (O) and compounds in which  $\text{Ti}^{4+}$  is fourfold, fivefold, and sixfold coordinated by O. The maximum of the preedge feature for metallic Ti is used for monochromator energy calibration (maximum set at 4966.8 eV).

### XANES spectroscopy

To calibrate Ti *K*-edge XANES spectra for the metamict minerals, many model compounds containing  $^{47}\text{Ti}$ ,  $^{48}\text{Ti}$ , and  $^{49}\text{Ti}$  were investigated (a select listing of them is given in Table 1). Detailed information about their structures and origins (or synthesis) is given elsewhere (Farges et al. 1996a). Ti *K*-edge XANES spectra were collected at the LURE facility (Laboratoire pour l'Utilisation du Rayonnement Electromagnétique, Orsay, France). The DCI storage ring was operated at 1.8 GeV and 100–300 mA positron current. XANES data were collected at the Ti *K* edge (4966 eV) using a high-resolution transmission mode [Si(311) double-crystal monochromator and 0.3 mm vertical slit before the monochromator] on beam station EXAFS4. The maximum of the preedge for metallic titanium was used for monochromator energy calibration following international recommendations (maximum set at 4966.8 eV; see Fig. 1). Energy resolution was estimated to be ~1.2 eV at 5 keV in these conditions (see details in Farges et al. 1996a). Preedge parameters (absolute position and height relative to the edge jump; Table 1) was extracted from the normalized spectra by fitting Lorentzian profiles to these features.

## RESULTS

### Preedge features for model compounds

The Ti *K*-edge XANES spectra collected for oxide-type model compounds show some preedge features, located ~18 eV before the main-edge crest (Fig. 1). These features are commonly attributed to electronic transitions from 1s energy levels of Ti to the Ti 3d or O 2p molecular orbitals (Waychunas 1987; Farges et al. 1996a). A 1s  $\rightarrow$  3d transition is forbidden by dipole selection rules but is allowed when p-d orbital mixing occurs, such as when Ti is located in a noncentrosymmetric site (e.g., a  $\text{TiO}_4$  tetrahedron). At

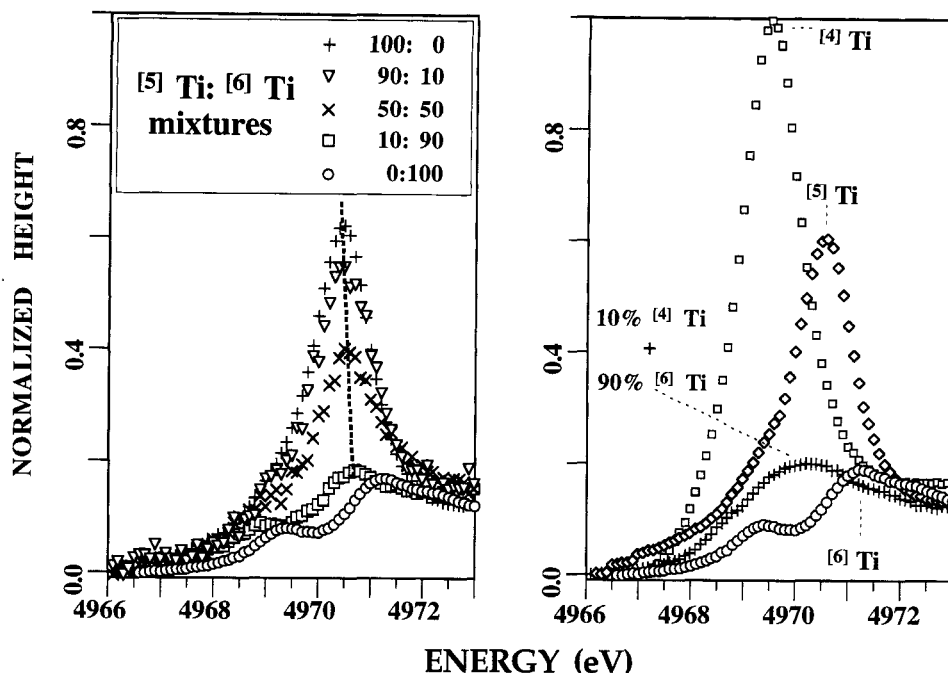


FIGURE 2. Strengths and limitations of the protocol used in this study. (left) Measured variation of the preedge feature for several mechanical mixtures of  $^{51}\text{Ti}$  (as  $\text{Ba}_2\text{TiGe}_2\text{O}_8$ ) and  $^{60}\text{Ti}$  (as  $\text{TiZrO}_4$ ). The detection level for each Ti coordination is  $\sim 10$  at%. (right) Examples of preedge features measured for  $^{44}\text{Ti}$ ,  $^{51}\text{Ti}$ , and  $^{60}\text{Ti}$ , in comparison with a preedge feature measured for a me-

chanical mixture of  $\sim 10$  at%  $^{44}\text{Ti}$  and  $\sim 90$  at% of  $^{60}\text{Ti}$ . Note that the preedge for the mixture has an energy position that is close to that for  $^{51}\text{Ti}$  (see also Fig. 4), but the preedge feature for the mixture is much broader. This difference favors the presence of  $^{51}\text{Ti}$  in the metamict state of zirconolite and eliminates the possibility of a mixture between  $^{44}\text{Ti}$  and  $^{60}\text{Ti}$ .

constant oxidation state and experimental resolution, the height and position of the preedge feature are direct functions of the degree of p-d mixing, i.e., the geometry of the  $\text{Ti}^{4+}$  coordination environment. Three well-separated domains for the preedge parameters can be identified for  $^{44}\text{Ti}$ ,  $^{51}\text{Ti}$ , and  $^{60}\text{Ti}$ , respectively (Table 1). The preedge features are found to have the greatest height for  $^{44}\text{Ti}$  (e.g., as high as 100% of the edge jump), whereas those for  $^{60}\text{Ti}$  are shifted to higher energies in comparison with  $^{44}\text{Ti}$  (by  $\sim 2 \pm 0.2$  eV; Table 1). Preedge energies and heights for  $^{51}\text{Ti}$  fall between the values measured for the other two Ti coordinations. The use of both preedge parameters is necessary to determine coordination reliably from preedge features collected in compounds containing different Ti coordinations. For instance, the use of both parameters allows the distinction between  $^{51}\text{Ti}$  and a 50:50 mixture of  $^{44}\text{Ti}$  and  $^{60}\text{Ti}$  (Fig. 2). Finally,  $^{44}\text{Ti}$  and  $^{51}\text{Ti}$  show just one noticeable preedge feature. In contrast,  $^{60}\text{Ti}$  is characterized by the presence of two to three preedge features (the most intense feature was used to measure the preedge height, following Waychunas 1987).

#### Preedge features for crystalline and metamict titanite and zirconolite

The Ti preedge parameters for crystalline titanite (Table 1; Fig. 3) are typical of  $^{60}\text{Ti}$  (similar to those of anatase), in good agreement with crystal-structure data

(Speer and Gibbs 1976). Preedge parameters for crystalline zirconolite lie near the domain for  $^{60}\text{Ti}$  (especially the preedge height). But the preedge position ( $4970.9 \pm 0.1$  eV) is low in comparison with all other  $^{60}\text{Ti}$ -bearing model compounds studied (average is  $4971.4 \pm 0.3$  eV). According to Figure 4, this preedge position may be due to the presence of some significant amount of low coordination around Ti ( $^{51}\text{Ti}$ ,  $^{44}\text{Ti}$ , or both; in this case, XANES cannot clearly differentiate between  $^{51}\text{Ti}$  and  $^{44}\text{Ti}$ , but, in all cases,  $^{60}\text{Ti}$  is dominant). Indeed, crystalline zirconolite contains one-third of the total Ti as  $^{51}\text{Ti}$  (the other two-thirds being  $^{60}\text{Ti}$ ) (Gatehouse et al. 1981).

The Ti  $K$ -edge XANES spectra collected for the metamict zirconolite and titanite samples are identical to those previously published (Ewing et al. 1988; Hawthorne et al. 1991). The preedge information for the two highly metamict zirconolite samples are significantly different in comparison with their crystalline counterpart (especially in position): This feature falls on the lower side of the domain for  $^{51}\text{Ti}$  (Fig. 4), suggesting that some significant amount of a lower Ti coordination is present in the two radiation-damaged samples.

The preedge parameters for the slightly damaged titanite from Ontario is shifted toward lower energies than that measured for its crystalline counterpart from Brazil (by  $0.3 \pm 0.1$  eV). Also, the normalized height increases slightly from 0.18 to  $0.27 \pm 0.05$  (Figs. 3 and 4). In comparison

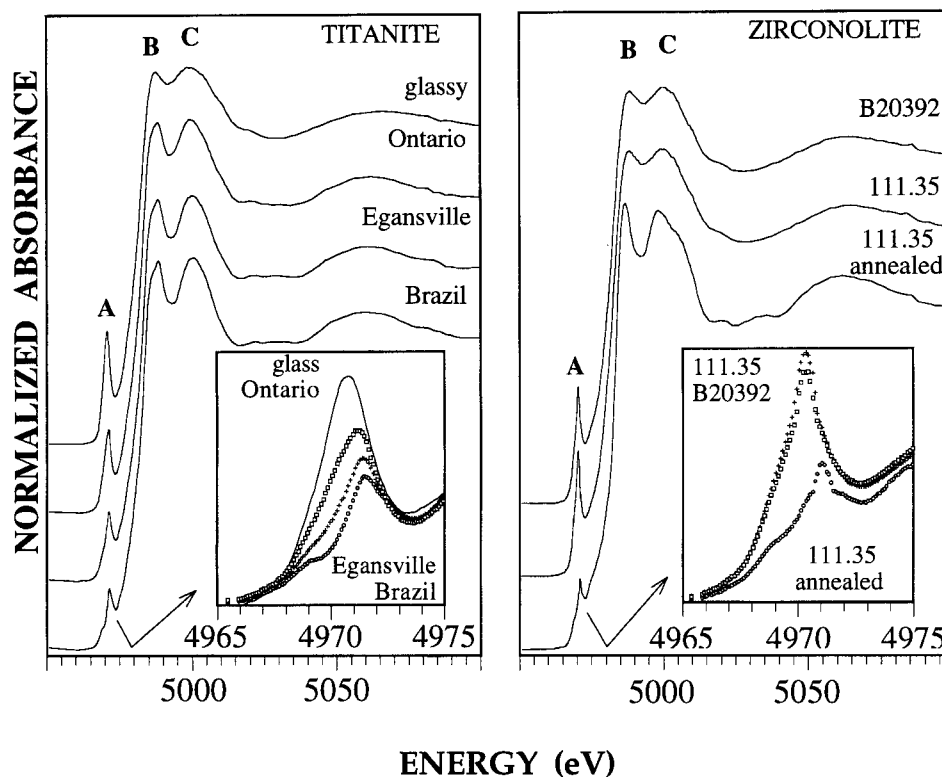


**FIGURE 3.** Ti *K*-edge XANES spectra collected for the four titanite samples ( $\text{CaTiSiO}_5$ ; **left**) and the three zirconolite samples ( $\text{CaZrTi}_2\text{O}_7$ ; **right**), showing variable degrees of aperiodicity: crystalline (Brazil), radiation damaged (Egansville and Ontario), and glassy (top spectrum). The loss of long- and medium-range structure broadens the two edge crests (B and C), whereas the preedge (A) shifts to a position and a height that are typical of mixtures of  $^{16}\text{Ti}$  and  $^{15}\text{Ti}$ . Metamict titanite samples are only partially metamict, whereas the metamict zirconolite samples are fully aperiodic.

with crystalline titanite, the change in the preedge feature is insignificant for the Egansville titanite. In contrast, the preedge feature for the Ontario titanite is shifted toward lower energies by  $0.3 \pm 0.1$  eV and has a greater height (by  $9 \pm 5\%$ ) than crystalline titanite (see Table 1).

### DISCUSSION

The preedge position observed for the two metamict zirconolite samples ( $4970.5 \pm 0.1$  eV) is indicative of a variety of mixtures between  $^{15}\text{Ti}$  and  $^{16}\text{Ti}$  containing  $>50\%$   $^{15}\text{Ti}$  (see Fig. 4). However, this preedge position can also be explained by a particular mixture of  $^{14}\text{Ti}$  and  $^{16}\text{Ti}$  (in the fixed proportions:  $5:95 \pm 1$ ; Fig. 4). However, it would be an exceptional coincidence for both samples to show this very particular mixture (most of the  $^{14}\text{Ti}$ - $^{16}\text{Ti}$  mixtures have a much lower preedge energy, i.e., well below 4970.0 eV). Also, a mixture of  $^{14}\text{Ti}$  and  $^{16}\text{Ti}$  would broaden the preedge feature significantly (see Fig. 2), which was not observed. A shift in the preedge position can also be attributed to the presence of  $\text{Ti}^{3+}$  (Waychunas 1987). However, this is unlikely because ionizing radiations would be expected to oxidize radioactive materials. Also, the presence of  $\text{Ti}^{3+}$  would be expected to shift the entire XANES spectrum toward lower energy, which was not observed.

Therefore, a preedge position at  $4970.5 \pm 0.1$  eV is indicative of the presence of  $^{15}\text{Ti}^{4+}$  in metamict zirconolite.

The calculation of the amount of  $^{15}\text{Ti}$  relative to  $^{16}\text{Ti}$  in these radiation-damaged samples is difficult because the preedge features for both  $^{15}\text{Ti}$  and  $^{16}\text{Ti}$  in metamict zirconolite are unknown. To get some indication of the amounts of both coordinations in metamict zirconolite, we used two methods. The first method is based on Figure 4, which shows preedge parameters determined for a variety of mechanical mixtures of  $^{15}\text{Ti}$  and  $^{16}\text{Ti}$ , assuming average values for the preedge parameters for these two coordinations ( $4970.6$  and  $4971.4$  eV for the energy,  $0.55$  and  $0.20$  for the height, respectively). On the basis of this figure, the preedge height and position for metamict zirconolite correspond to a  $60:40 \pm 20$  mixture between these two coordinations. This method has the advantage of being simple and is based on a statistical approach of preedge analysis.

There is another method for deriving the respective amounts of  $^{15}\text{Ti}$  and  $^{16}\text{Ti}$  in metamict zirconolite that is probably better adapted to zirconolite compounds. We first examine the case of crystalline zirconolite, for which it is known from X-ray diffraction that there are three non-equivalent sites for Ti: One is occupied by  $^{15}\text{Ti}$  in a trigonal

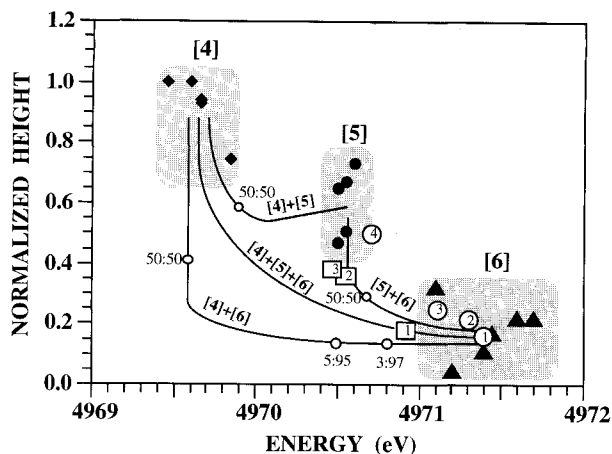


**FIGURE 4.** Normalized preedge height vs. preedge energy position for the preedge features at the Ti K edge in Ti-bearing model compounds (Table 1) and in the four titanite samples (circles: 1 = crystalline from Caperlibas, Brazil; 2 = partially damaged from Egansville, Ontario; 3 = partially damaged from an unknown locality, Ontario; 4 = glassy synthetic titanite) and the three zirconolite samples (squares: 1 = annealed 111.35; 2 = fully metamict 111.35; 3 = fully metamict B-20392). The domains for  $^{47}\text{Ti}$ ,  $^{51}\text{Ti}$ , and  $^{67}\text{Ti}$  are shown, labeled [4], [5], and [6]. The variation of the preedge parameters for mixtures of coordinations (along the paths shown as solid lines) and the preedge parameters for some particular mixtures [open circles; see Farges et al. (1996a) for details] are also shown. For instance, see the difference between the preedge parameters for  $^{51}\text{Ti}$  and those of a 50:50 mixture of  $^{47}\text{Ti}$  and  $^{67}\text{Ti}$ .

bipyramid, and two are occupied by  $^{67}\text{Ti}$  in octahedral geometry (Gatehouse et al. 1981; Mazzi and Munno 1983; Cheary 1992). We previously found distinct ranges of values for the preedge energy ( $4970.6 \pm 0.1$  and  $4971.4 \pm 0.3$  eV) and height (0.55 and  $0.20 \pm 0.15$ ) for  $^{51}\text{Ti}$  and  $^{67}\text{Ti}$  in a variety of model compounds (Table 1). Also, the preedge information for each coordination shows relatively moderate variations:  $\pm 0.1$  ( $^{51}\text{Ti}$ ) to  $\pm 0.3$  eV ( $^{67}\text{Ti}$ ) for the energy and  $\pm 0.15$  for the height, respectively (see Table 1). On the basis of these ranges of values, the contributions arising from each Ti coordination present in crystalline zirconolite (e.g.,  $^{51}\text{Ti}$  and  $^{67}\text{Ti}$  in the proportion 1:2) can be estimated relatively accurately by interpolation. During the calculation, the preedge positions for both coordinations were fixed at the average values for  $^{51}\text{Ti}$  and  $^{67}\text{Ti}$  (4970.6 and 4971.4 eV, respectively) because these parameters show the smallest variations. In contrast, the preedge heights were allowed to vary within their respective limits (0.4–0.7 and 0.05–0.35) until the preedge feature for the mixture (one-third  $^{51}\text{Ti}$  and two-thirds  $^{67}\text{Ti}$ ) fitted the measured preedge spectrum for crystalline zirconolite (Fig. 5, left). The refined preedge heights for  $^{51}\text{Ti}$  and  $^{67}\text{Ti}$  are  $\sim 0.45$  (such as in  $\text{Rb}_2^{51}\text{Ti}_4\text{O}_9$ ) and  $0.13 \pm 0.05$  (such as in  $\text{Ca}^{67}\text{TiO}_3$ , perovskite), respectively. The preedge parameters determined for the nonequivalent site occupied by  $^{51}\text{Ti}$  in crystalline zirconolite are the first estimates for  $^{51}\text{Ti}$  in a trigonal bipyramidal geometry (indeed, all other  $^{51}\text{Ti}$ -bear-

ing oxide model compounds reported in the literature show Ti in a square pyramidal environment). Thus, this method is particularly well suited to zirconolite, in which  $^{51}\text{Ti}$  is located in an unusual trigonal bipyramid. On the basis of these estimates for  $^{51}\text{Ti}$  and  $^{67}\text{Ti}$  in crystalline zirconolite, one can reconstruct the variation of preedge parameters for any mechanical mixture of these two particular coordinations (Fig. 5, right). Using this model, we derived the relative proportions of  $^{51}\text{Ti}$  and  $^{67}\text{Ti}$  in the metamict counterpart. This calculation assumes that  $^{51}\text{Ti}$  occurs as trigonal bipyramids in metamict zirconolite (we demonstrate below that this model is plausible, on the basis of EXAFS data). On the basis of Figure 5 (right side), the preedge height measured in the radiation-damaged samples (0.36–0.39) suggests that  $\sim 80$ – $90(\pm 5)\%$  of the total Ti is present as  $^{51}\text{Ti}$ . This estimate is consistent with that previously calculated using a less sophisticated method ( $60 \pm 20\%$ ). For both models,  $^{51}\text{Ti}$  is a major coordination in metamict zirconolite, if not the dominant one.

#### Evidence for trigonal bipyramidal coordination of $^{51}\text{Ti}$ in metamict zirconolite

In oxide-type compounds,  $^{51}\text{Ti}^{4+}$  is present mostly in square pyramidal coordination (fresnoite, lamprophyllite, innelite,  $\text{KNaTiO}_3$ , Ti-bearing glasses; see review in Farges et al. 1996a). Trigonal bipyramids are documented essentially in crystalline zirconolite. Because of the close structural relationships between crystalline and metamict zirconolite (see discussion in Farges et al. 1993), trigonal bipyramids may also occur in the aperiodic regions of metamict zirconolite. This suggestion is consistent with the analysis of the EXAFS data collected at the Ti K edge in metamict “blomstrandine” [= aeschynite-(Y), or  $(\text{Ce,Ca,Fe,Th,Y})(\text{Ti,Nb})_2(\text{O,OH})_6$ ; Gregor et al. 1984a, 1984b]. These compounds have preedge and XANES spectra at the Ti K edge that are very similar to that collected for the fully metamict 111.35 zirconolite (see Ewing et al. 1988). Therefore, the previous discussion about the importance of  $^{51}\text{Ti}$  in metamict zirconolite may also apply to the metamict titanium oxides. Also, in metamict blomstrandine, Gregor et al. (1984b) fitted the EXAFS-derived Ti-O contribution with four shells of Ti-O distances centered around  $\sim 1.81(2)$  (2.2 O atoms around Ti), 1.91 (2.8 O atoms), 2.07 (0.3 O atoms), and 2.16 Å (0.2 O atoms). This set of Ti-O distances averages 1.89 Å, which is typical for  $^{51}\text{Ti}$  (the predicted average  $^{51}\text{Ti}$ -O distance, on the basis of ionic radii, is 1.91 Å). This result confirms that  $^{51}\text{Ti}$  can be dominant in these metamict minerals, in good agreement with the preedge parameters. In addition, this Ti-O distance distribution is inconsistent with the square pyramidal geometry, which is characterized by one short Ti=O double bond (bond length between 1.69 and 1.78 Å) and four longer Ti-O bonds (between 1.9 and 2.0 Å). In contrast, the Ti-O distance distribution in metamict blomstrandine is not far from that known for the trigonal bipyramids around  $^{51}\text{Ti}$  in crystalline zirconolite ( $2 \times \text{O}$  at 1.79,  $1 \times \text{O}$  at 1.81,  $1 \times \text{O}$  at 2.19, and  $1 \times \text{O}$  at 2.25 Å; Gatehouse et al. 1981).

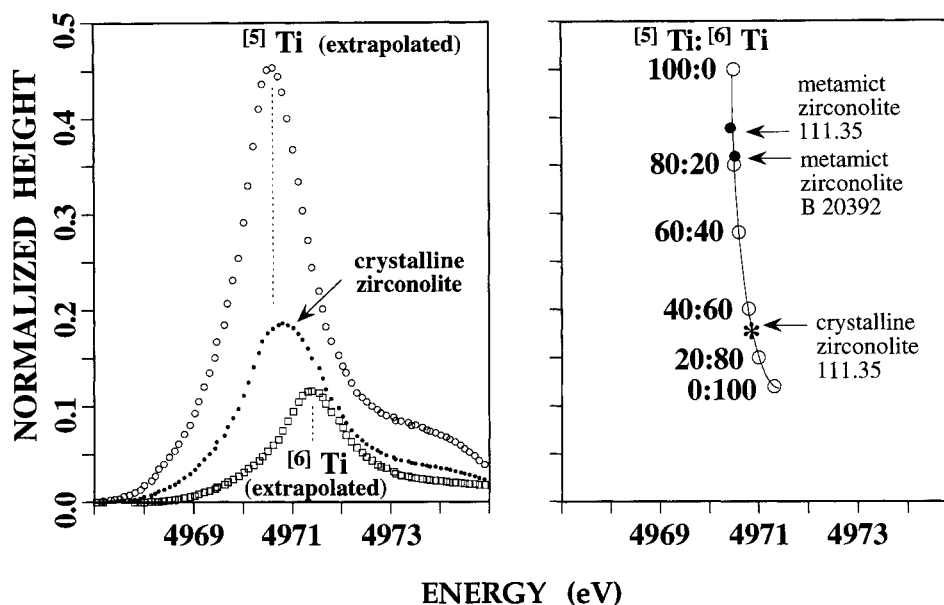


**FIGURE 5.** (left) The best model of mixture between  $^{51}\text{Ti}$  and  $^{61}\text{Ti}$  obtained for the most intense preedge feature in crystalline zirconolite (one site for  $^{51}\text{Ti}$  and two sites for  $^{61}\text{Ti}$ ; solid circles). The spectrum shown for crystalline zirconolite corresponds to a Lorentzian simulating the most intense feature observed in the experimental preedge spectrum for crystalline zirconolite (see text; this protocol minimizes the influence of the other preedge components observable in the experimental spectrum for zirconolite; see Fig. 3). The calculated preedge for  $^{51}\text{Ti}$  (open circles,

preedge position fixed at 4970.6 eV) has a height of  $\sim 0.45$ , whereas that for  $^{61}\text{Ti}$  (open squares, preedge position fixed at 4971.4 eV) is  $\sim 0.13$ . (right) On the basis of the two preedges determined in the figure on the left, preedge parameters were calculated for all mixtures between 100%  $^{51}\text{Ti}$  (mixture 100:0) and 100%  $^{61}\text{Ti}$  (mixture 0:100). According to that particular model, the preedge parameters for the two metamict zirconolite samples suggest that  $>80\text{--}90\%$  of Ti in these minerals is present as  $^{51}\text{Ti}$ .

A very similar conclusion can be drawn for metamict pyrochlore (XAFS data in Ewing et al. 1988). Thus, according to these models,  $^{51}\text{Ti}^{4+}$  is probably located within trigonal bipyramids in metamict titanium oxides (zirconolite, aeschynite, and pyrochlore).

#### Evidence for some $^{51}\text{Ti}$ in metamict titanite?

The preedge parameters for metamict titanite lie within the domain of values for  $^{61}\text{Ti}$ , suggesting the presence of significant amounts of  $^{61}\text{Ti}$  in these samples. In glassy titanite, the preedge feature suggests major amounts of  $^{51}\text{Ti}$  (but as square pyramids; Farges et al. 1996b). In comparison with crystalline titanite, the preedge parameters for the metamict samples are shifted in a direction (lower energy, greater height) that suggests either the presence of a more distorted  $^{61}\text{Ti}$  site (Waychunas 1987) (as in neptunite; see Fig. 1 and Table 1), a greater proportion of  $^{51}\text{Ti}$ , or both. With the current data, it is difficult to distinguish between the two models. However, increasing metamictization in titanite shifts the preedge feature in a similar way to that observed for zirconolite, suggesting that radiation damage also favors the presence of  $^{51}\text{Ti}$ . If this model is correct, the amount of  $^{51}\text{Ti}$  (over  $^{61}\text{Ti}$ ) increases clearly with increasing radiation dose (e.g., in the order Caperlibas < Egansville < Ontario  $\ll$  B-20392 < 111.35).

Ti *K*-edge EXAFS spectroscopy data for a metamict titanite from the Cardiff mine (Ontario) has suggested the appearance of 0.2 O-atom first neighbors near 1.81 Å in comparison with crystalline titanite (Hawthorne et al. 1991). This result is interpreted as indicative of the presence of minor amounts of  $^{41}\text{Ti}$  (e.g.,  $\sim 0.2$  atoms or  $\sim 3\%$  of the total Ti). For such a mixture, the preedge feature should be broader and centered near  $4970.8 \pm 0.1$  eV, which was not observed (Fig. 4). A Ti-O contribution near 1.81 Å can also result from  $^{51}\text{Ti}$  (a possible short Ti-O distance around  $\text{Ti}^{4+}\text{O}_5$ , trigonal bipyramids). EXAFS data for highly damaged titanite samples would give more reliable conclusions (unfortunately, such samples were not available for this study).

#### Implications for the coordination chemistry of Ti in aperiodic materials

Fivefold-coordinated  $\text{Ti}^{4+}$  should now be recognized as an important coordination in radiation-damaged oxides and silicates. Examination of the preedge parameters at the Ti *K* edge in a variety of highly metamict titanium-niobium-tantalum oxides such as euxenite, aeschynite, betafite, and pyrochlore (Greegor et al. 1984a, 1984b; Ewing et al. 1988) suggests that the coordination chemistry of Ti in these highly metamict minerals is similar to that observed in the two fully metamict zirconolite samples studied here.

The height of the preedge features of these complex metamict oxides (especially pyrochlore and zirconolite) is much greater than that of their crystalline counterparts. More important, the preedge positions for the metamict modifications are all shifted toward lower energies (by  $\sim 0.5$ – $1$  eV, as for metamict zirconolite). These changes can be attributed to the presence of major amounts of  $^{51}\text{Ti}$ . This analysis of the preedge parameters is then consistent with the EXAFS data for metamict pyrochlore (Greggor et al. 1984a, 1984b; Ewing et al. 1988), which can also be explained by the presence of  $^{51}\text{Ti}^{4+}$  as trigonal bipyramids. Here again, large amounts for  $^{51}\text{Ti}$  are found in the most radiation-damaged samples.

The change in coordination number of Ti from five to six that is induced by  $\alpha$ -recoil damage in several Ti-bearing minerals must dramatically affect the local structure around Ti in these radiation-damaged materials. In contrast, the coordinations of  $\text{Zr}^{4+}$  and  $\text{Th}^{4+}$  in metamict zirconolite (sevenfold and eightfold, respectively) are little affected by radiation damage (Farges et al. 1993). This comparison shows some structural similarities between the crystalline and the metamict modifications (Zr, Th) but also emphasizes some fundamental differences (Ti).

Finally, the metamict titanium oxides may be an example of a rare class of minerals in which trigonal pyramids around  $\text{Ti}^{4+}$  are present, as in crystalline zirconolite (Gatehouse et al. 1981). This environment is much different from that determined for a variety of Ti-bearing oxide glasses and melts, in which  $^{51}\text{Ti}^{4+}$  is also found but as square pyramids (see Farges et al. 1996b). Because glasses are quenched from high-temperature melts, square pyramidal  $\text{Ti}^{4+}$  may be a high-temperature species that could be metastable at room temperature in the glassy state. In contrast, radiation damage occurs at much lower temperatures and promotes highly disordered structures with complex medium-range environments. This observation contrasts with that for titanosilicate glasses, in which a relatively more ordered medium-range structure can be detected around Ti (see Farges et al. 1996b). Therefore, these high-resolution Ti *K*-edge XANES data provide another example of structural similarities between various types of aperiodic materials but also highlight some differences between the glassy and the metamict states.

#### ACKNOWLEDGMENTS

The author is indebted to H.J. Schubnel, R.C. Ewing, A. Voileau, J.S. White, and G.E. Brown Jr. for donating the samples used in this study, and to the staff of LURE for their help in data collection. R.C. Ewing and an anonymous reviewer are thanked for their helpful reviews of this manuscript.

#### REFERENCES CITED

- Cheary, R.W. (1992) Zirconolite  $\text{CaZr}_{0.92}\text{Ti}_{2.08}\text{O}_7$  from 294 to 1173 K. *Journal of Solid State Chemistry*, 98, 323–329.
- Ewing, R.C., Haaker, R.F., Headley, T.J., and Hlava, P.F. (1982) Zirconolites from Sri-Lanka, South Africa and Brazil. In S.V. Topp, Ed., *Scientific basis for nuclear waste management*, vol. 6, p. 249–256. North Holland, New York.
- Ewing, R.C., Chakoumakos, B.C., Lumpkin, G.R., and Murakami, T. (1987) The metamict state. *Material Research Society Bulletin*, 12, 58–66.
- Ewing, R.C., Chakoumakos, B.C., Lumpkin, G.R., Murakami, T., Greggor, R.B., and Lytle, F.W. (1988) Metamict minerals: Natural analogues for radiation damage effects in ceramic nuclear waste forms. *Nuclear Instruments and Methods in Physics Research B*, 32, 487–497.
- Ewing, R.C., Weber, W.J., and Clinard, F.W., Jr. (1995) Radiation effects in nuclear waste forms for high-level radioactive waste. *Progress in Nuclear Energy*, 29, 63–127.
- Farges, F., Ewing, R.C., and Brown, G.E., Jr. (1993) The structure of metamict, aperiodic  $(\text{Ca,Th})_2\text{Zr}_2\text{Ti}_2\text{O}_{14}$ . *Journal of Material Research*, 8, 1983–1995.
- Farges, F., Brown, G.E., Jr., and Rehr, J.J. (1996a) Coordination chemistry of Ti(IV) in silicate glasses and melts: I. XAFS study of titanium coordination in oxide model compounds. *Geochimica et Cosmochimica Acta*, 60, 3023–3038.
- Farges, F., Brown, G.E., Jr., Navrotsky, A., Gan, H., and Rehr, J.J. (1996b) Coordination chemistry of Ti(IV) in silicate glasses and melts: III. Glasses and melts from ambient to high temperatures. *Geochimica et Cosmochimica Acta*, 60, 3055–3065.
- Fleet, M.E., and Henderson, G.S. (1985) Radiation damage in natural titanite by crystal structure analysis. *Material Research Society Symposium Proceedings*, 50, 363–370.
- Gatehouse, B.M., Grey, I.E., Hill, R.J., and Rossell, H.J. (1981) Zirconolite,  $\text{CaZrTi}_{1-x}\text{O}_7$ : Structure refinements for near-end member compositions with  $x = 0.85$  and  $1.3$ . *Acta Crystallographica*, B37, 306–312.
- Greggor, R.B., Lytle, F.W., Ewing, R.C., and Haaker, R.F. (1984a) Ti-site geometry in metamict, annealed and synthetic complex Ti-Nb-Ta oxides by X-ray absorption spectroscopy. *Nuclear Instruments and Methods in Physics Research B*, 1, 587–594.
- (1984b) EXAFS/XANES studies of metamict minerals. In K.O. Hodgson, B. Hedman, and J.E. Penner-Hahn, Eds., *EXAFS and near-edge structure III*, vol. 2, p. 343–348. Springer Verlag, New York.
- Hawthorne, F.C., Groat, L.A., Raudsepp, M., Ball, N.A., Kimata, M., Spike, F.D., Gaba, R., Halden, N.M., Lumpkin, G.R., Ewing, R.C., Greggor, R.B., Lytle, F.W., Ercit, T.S., Rossman, G.R., Wicks, F.J., Ramik, R.A., Sherriff, B.L., Fleet, M.E., and McCammon, C. (1991) Alpha-decay damage in titanite. *American Mineralogist*, 76, 370–396.
- Higgins, J.B., and Ribbe, P.H. (1976) The crystal chemistry and space groups of natural and synthetic titanites. *American Mineralogist*, 61, 878–888.
- Lumpkin, G.R., Ewing, R.C., Chakoumakos, B.C., Greggor, R.B., Lytle, F.W., Foltyn, E.M., Clinard, F.W., Jr., Boatner, L.A., and Abraham, M.M. (1986) Alpha-recoil damage in zirconolite ( $\text{CaZrTi}_2\text{O}_7$ ). *Journal of Material Research*, 1, 564–576.
- Lumpkin, G.R., Eby, R.K., and Ewing, R.C. (1991) Alpha-recoil damage in titanite ( $\text{CaTiSiO}_6$ ): Direct observation and annealing study using high resolution transmission electron microscopy. *Journal of Material Research*, 6, 560–564.
- Lutze, W., and Ewing, R.C. (1988) Summary and evaluation of nuclear waste forms. In W. Lutze and R.C. Ewing, Eds., *Radioactive waste forms for the future*, p. 700–740. Elsevier, Amsterdam.
- Mazzi, F., and Munno, R. (1983) Calciobetafite (new mineral of the pyrochlore group) and related minerals from Campi Flegrei, Italy, crystal structure of polymignyte and zirkelite: Comparison with pyrochlore and zirconolite. *American Mineralogist*, 68, 262–276.
- Ringwood, A.E., Kesson, S.E., Reeve, K.D., Levins, D.M., and Ramm, E.J. (1988) Synroc (for radwaste solidification). In W. Lutze and R.C. Ewing, Eds., *Radioactive waste forms for the future*, p. 233–334. North-Holland, Amsterdam.
- Speer, J.A., and Gibbs, G.V. (1976) The crystal structure of synthetic titanite,  $\text{CaTiOSiO}_6$ , and the domain textures of natural titanites. *American Mineralogist*, 61, 238–247.
- Vance, E.R., and Metson, J.B. (1985) Radiation damage in natural titanites. *Physics and Chemistry of Minerals*, 12, 255–260.
- Waychunas, G.A. (1987) Synchrotron radiation XANES spectroscopy of Ti in minerals: Effects of Ti bonding distances, Ti valence, and site geometry on absorption edge structure. *American Mineralogist*, 72, 89–101.